Numerical and Experimental Investigations for Effect of Gravity to the Heat Transfer and Fluid Flow Phenomena of Microchannel Heat Exchangers

Thanhtrung Dang[1,*], Ngoctan Tran[2], and Jyh-tong Teng[2]

[1] Department of Heat and Refrigeration Technology, Ho Chi Minh City University of Technical Education, Ho Chi Minh City, Vietnam

[2] Department of Mechanical Engineering, Chung Yuan Christian University, Taiwan

Abstract

For both numerically and experimentally, effect of gravity on the heat transfer and fluid flow phenomenon of microchannel heat exchangers was presented. The influence was determined by two cases: one with horizontal channels, the other with vertical channels. For vertical channels, the hot water is flowing upward which is against the gravitational field, while the cold water is flowing downward which is in the same direction as the gravitational field. In this study, the difference between the results obtained from horizontal channels and those from vertical ones is negligibly small; the impact of gravity on the fluid through the microchannel heat exchangers was found to be small, with the maximum difference between the two cases being less than 8%. The results obtained from numerical simulation and experimental data are in good agreement. In addition, good agreements were also achieved between the results obtained in the present study and the results obtained in literatures.

Keywords: micro heat exchanger, gravity, heat transfer rate, pressure drop, performance index.

I. INTRODUCTION

The development of effective cooling devices has promoted attractive area of study in microchannel heat transfer in recent years. A review on micro heat exchangers was done by Dang et al. [1] with five sections. The first section dealt with the single-phase micro heat exchangers which consist of the micro channel heat exchangers as well as the micro porous/foam heat exchangers. The second section reviewed the two-phase micro heat exchangers which consist of micro evaporators and micro condensers. The third section dealt with micro heat exchangers for carbon dioxide air conditioning system. The fourth section reviewed optimization of micro heat exchanger. The last section dealt with other types of micro heat exchangers. David et al. [2] studied hydraulic and thermal characteristics of a vapor venting two-phase microchannel heat exchanger. They found 60% improvement in the normalized pressure drop and up to 4.4 °C reduction in the average substrate temperature between the control and vapor venting device under similar operating conditions.

Brandner et al. [3] described microstructure heat exchangers and their applications in laboratory and industry. Several micro heat exchangers were introduced: polymer microchannel heat exchanger with aluminum separation foil, electrically powered lab-scale microchannel evaporator, ceramic counter-flow microstructure heat exchanger, etc. Ameel et al. [4] presented an overview of the miniaturization technologies and their applications to energy systems. Based on the MEMS technologies (silicon-based micromachining, deep X-ray lithography, and the micro mechanical machining), processes were discussed in the context of applications to fluid flow, heat transfer, and energy systems. Review on experimental results concerning single-phase convective heat transfer in microchannels was presented by Morini [5], with additional review results obtained for the friction factor, the laminar-to-turbulent transition, and the Nusselt number in channels having a hydraulic diameter less than 1 mm.

Mathew and Hegab [6] studied on the application of effectiveness-NTU relationship to parallel-flow microchannel heat exchangers. Besides, development of nondimensional parameters (such as axial distance, temperature, and heat transfer rate) was carrier out. However, the results were analyzed theoretically only. Studies of effectiveness and pressure drop for micro cross-flow heat exchanger were presented by Kang and Tseng [7]. At the same effectiveness, heat transfer rate and pressure drop were expressed as a function of average temperature. However, in their study, they did not study for the cases with varying mass flow rates at each side.

Chein and Chen [8] presented a numerical study of the effect of inlet/outlet arrangement on the performance of microchannel heat sink. Six types of heat sink were studied with the best performance being the V-type. Because that if the microchanels have the same cross-section area and width of microchannel, the depth of microchannel obtained from V-shaped microchannel is deeper than that obtained from rectangular-shaped one. So it is not easy to design a heat exchanger with the subtrate thickness from 1.2 to 2 mm using V-type microchannels. Foli et al. [9] studied numerically on the heat flux, heat transfer rate, and pressure drop in channels with numerous aspect ratios. However, the results in Ref. [9] were presented without experiments.

A study on the simulations of a trapezoidal shaped micro heat exchanger was presented by Dang et al. [10]. For the microchannel heat exchanger, behaviors of the temperature, heat flux, and velocity profiles were determined. Effect of flow arrangement on the heat transfer related behaviors of a microchannel heat exchanger was presented by Dang et al. [11, 12]. For all cases done in the study, the heat flux and performance index obtained from the counter-flow arrangement are always higher than those obtained from the parallel-flow one: the values obtained from the counter-flow are 1.1 to 1.2 times of those obtained from the parallel-flow. Dang and Teng [13] studied effect of the substrate thickness of counter-flow microchannel heat exchangers on the heat transfer behaviors. It was found that the actual heat transfer rate varies insignificantly with the substrate thicknesses varying from 1.2 to 2 mm. However, the results obtained in [13] only mentioned the heat transfer behaviors of the heat exchangers, while the fluid flow behaviors of the heat exchangers were not discussed. Dang et al. [14] presented an experimental study of the effects of gravity on heat transfer and pressure drop behaviors of a microchannel heat exchanger. However, the results in [14] were presented only for a microchannel heat exchanger evaluated under the condition of rising the inlet temperature for the hot side. Dang and Teng [15, 16] studied the effects of configurations on performance of the microchannel and minichannel heat exchangers. However, their study ignored the effects of gravity on the performance index of microchannel heat exchangers.

To summarize, it is goal of this paper to study the effects of gravity on the heat transfer and fluid flow characteristics of microchannel heat exchangers, for both numerically and experimentally. In the following section, two microchannel heat exchangers will be discussed under the condition of rising mass flow rate for the cold side.

II. METHODOLOGY

A. Mathematical model

The governing equations in this system consist of the continuity equation, momentum equations, and energy equation [17,18]. The equations can be expressed by

Continuity equation

$$\frac{\partial \rho}{\partial t}+u\frac{\partial \rho}{\partial x}+v\frac{\partial \rho}{\partial y}+w\frac{\partial \rho}{\partial z}+\rho\left[\frac{\partial u}{\partial x}+\frac{\partial v}{\partial y}+\frac{\partial w}{\partial z}\right]=0 \tag{1}$$

Momentum equations

$$\frac{\partial u}{\partial t}+u\frac{\partial u}{\partial x}+v\frac{\partial u}{\partial y}+w\frac{\partial u}{\partial z}=\rho g_x-\frac{1}{\rho}\frac{\partial p}{\partial x}+\frac{\mu}{\rho}\left(\frac{\partial^2 u}{\partial x^2}+\frac{\partial^2 u}{\partial y^2}+\frac{\partial^2 u}{\partial z^2}\right) \tag{2a}$$

$$\frac{\partial v}{\partial t}+u\frac{\partial v}{\partial x}+v\frac{\partial v}{\partial y}+w\frac{\partial v}{\partial z}=\rho g_y-\frac{1}{\rho}\frac{\partial p}{\partial y}+\frac{\mu}{\rho}\left(\frac{\partial^2 v}{\partial x^2}+\frac{\partial^2 v}{\partial y^2}+\frac{\partial^2 v}{\partial z^2}\right) \tag{2b}$$

$$\frac{\partial w}{\partial t}+u\frac{\partial w}{\partial x}+v\frac{\partial w}{\partial y}+w\frac{\partial w}{\partial z}=\rho g_z-\frac{1}{\rho}\frac{\partial p}{\partial z}+\frac{\mu}{\rho}\left(\frac{\partial^2 w}{\partial x^2}+\frac{\partial^2 w}{\partial y^2}+\frac{\partial^2 w}{\partial z^2}\right) \tag{2c}$$

For steady-state conditions, $\partial \boldsymbol{u}/\partial t = 0$; the boundary conditions of inlet flow are $u = 0$, $v = 0$, and $w = w_0$; the boundary conditions of outlet flow are $\mu(\nabla\boldsymbol{u} + (\nabla\boldsymbol{u})^T)\boldsymbol{n} = \boldsymbol{0}$ and $p = p_0$, where μ is dynamic viscosity, ρ is density, g is gravity force, $\boldsymbol{u}$ is velocity field, u is velocity in the x-direction, v is velocity in the y-direction, w is velocity in the z-direction, p is pressure, and p_0 is pressure at the outlet.

For the energy transport, the walls have no-slip conditions for velocity and temperature at the walls; these conditions are expressed by $\boldsymbol{u}_{wall} = 0$ and $T_{wall} = T_{fluid\ at\ wall}$, respectively, where T_{wall} is wall temperature.

The heat transfer equation for the energy transport within the fluid is:

$$\frac{\partial T}{\partial t}+u\frac{\partial T}{\partial x}+v\frac{\partial T}{\partial y}+w\frac{\partial T}{\partial z}=\frac{\lambda}{\rho c_p}\left(\frac{\partial^2 T}{\partial x^2}+\frac{\partial^2 T}{\partial y^2}+\frac{\partial^2 T}{\partial z^2}\right)+Q_i \tag{3}$$

For steady-state conditions, $\partial T/\partial t = 0$; the boundary condition of inlet flow is $T = T_0$; the boundary condition of outlet flow is convective flux, expressed by $\boldsymbol{n} \bullet (-\lambda\nabla T) = 0$; the thermal boundary condition of the bottom and top walls of the microchannel heat exchanger are assumed to be constant heat flux, expressed by $-\boldsymbol{n} \bullet (-\lambda\nabla T) = q_0$; and the four side-walls are insulated thermally, expressed by $\boldsymbol{n} \bullet q = 0$, where heat flux $q = -\lambda\nabla T + \rho C_p T\boldsymbol{u}$, T is temperature, c_p is specific heat at constant pressure, Q_i is internal heat generation, and λ is thermal conductivity.

B. Experimental set-up

Three major parts are used in the experimental system: the test section (the microchannel heat exchanger), syringe system, and overall testing loop, as shown in Fig. 1. In this study, two microchannel heat exchangers were tested. The heat transfer process of these devices is carried out between two liquids which are hot water and cold water; the hot and cold fluids are flowing in the opposite directions. Fig. 2 shows the dimensions of the test sections. The substrate material used for the heat exchangers is aluminum, with the thermal conductivity of 237 W/(mK), density of 2,700 kg/m^3, and specific heat at constant pressure of 904 J/(kgK).

For each microchannel heat exchanger, the top side for the hot water has 10 microchannels and the bottom side for the cold water also has 10 microchannels. The length of each microchannel is 32 mm. Microchannels have rectangular cross-section with the width and the depth being W_c and D_c, respectively. In a microchannel heat exchanger, all channels are connected by manifolds for the inlet and outlet of hot water and for those of cold water, respectively. The manifolds of the heat exchangers are of the same cross-sections: having a rectangular shape with a width of 3 mm and a depth of 300 μm.

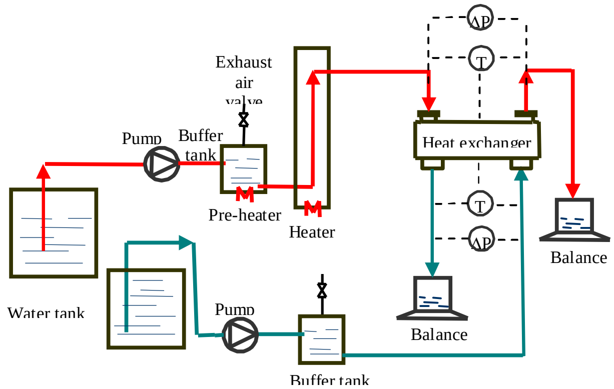

Fig. 1. Schematic of the test loop for microchannel heat exchangers

Table 1. Geometrical parameters of microchannel heat exchangers

No.	Dimensions of the substrate (mm)			Dimensions of the channel (μm)	
	L	W	T	W_c	D_c
T1	46	26.5	1.2	500	300
T2	46	26.5	1.2	500	180

Fig. 2 shows the dimensions of the test section. In this study, two microchannel heat exchangers were designed and manufactured, with their dimensions listed in Table 1. Fig. 3 shows a photo of the microchannel heat exchanger. These test sections were manufactured by precision micromachining [4]. Each inlet hole or outlet hole of the heat exchangers has a cross-sectional area of 9 mm^2. The four sides of the heat exchanger were thermally insulated by the glass wool with a thickness of 5 mm. To seal the microchannels, two layers of PMMA (polymethyl methacrylate) are bonded on the top and bottom sides of the substrate by UV (ultraviolet) light process, as indicated in Fig. 3. The physical properties of the PMMA and the glass wool are listed in Table 2 [17].

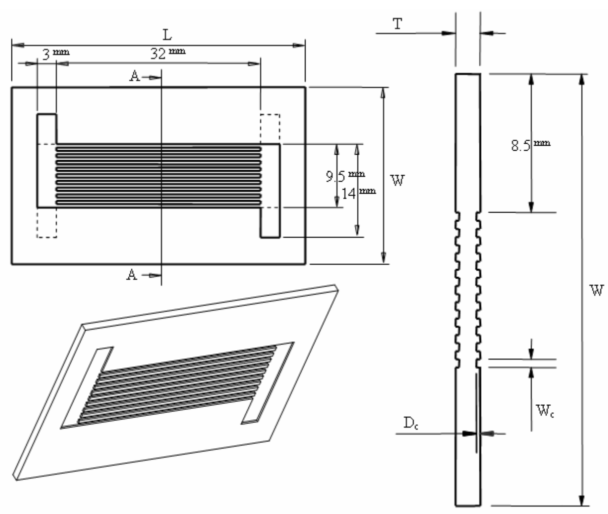

Fig. 2. Dimensions of the test section

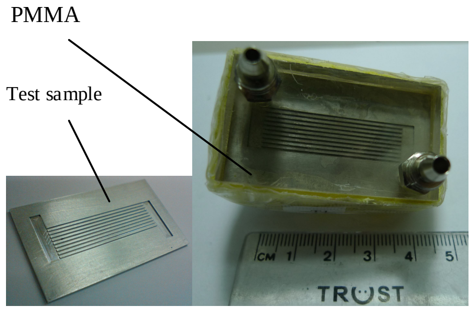

Fig. 3. A photo of the microchannel heat exchanger

Table 2. The physical properties of the PMMA and the glass wool

Material	Density kg/m^3	Thermal conductivity W/(mK)
PMMA	1420	0.19
Glass wool	154	0.051

Experimental data for the microchannel heat exchanger were obtained under the constant room temperature of 25 ºC. For this study, DI water (deionized water) was used as the working fluid. Each inlet or outlet of the heat exchanger has a set of two thermocouples to record temperature values. So, there are eight thermocouples in total. At each side, a differential pressure transducer was used to measure the pressure drop. To assess the accuracy of measurements presented in this work, the uncertainty values for measured parameters are listed in Table 3. In addition, the uncertainties on the dimensions of microchannel evaluated by using a scanning laser made by Mitaka/Ryokosha model NH-3. The uncertainties of the scanning laser were estimated to be $\pm$ 0.03 μm. Equipments used for the experiments are listed as follows [13-16]:

1. Thermocouples, T-type
2. Pump, Model PU-2087, made by Jasco
3. Pump, VSP-1200, made by Tokyo Rikakikai
4. Heater, Model AXW-8, made by Medilab
5. Differential pressure transducer, Model PMP4110, made by Duck
6. Micro electronic balance, Model TE-214S, made by Sartorious.

Table 3. Uncertainty data for measured parameters

Parameter	Uncertainties
Temperature	$\pm$ 0.1 °C
Pressure	$\pm$ 0.025% FS
Mass flow rate	$\pm$ 0.0015 g
Channel height	$\pm$ 7 μm
Channel width	$\pm$ 10 μm
Channel length	$\pm$ 70 μm

In order to study the effects of gravity on heat transfer and fluid flow behaviors of the heat exchangers, all experimental conditions for the two microchannel heat exchangers were kept the same. Throughout the paper, the experimental conditions of testing were discussed: the case is studied under condition of increasing the mass flow rate of the cold side. Further details of the case are as follows:

The inlet temperature and the mass flow rate of the hot side were fixed at 70 ºC and 0.2308 g/s, respectively; at the cold side, the inlet temperature was fixed at 22.5 ºC and the mass flow rates were varying from 0.2135 to 0.401 g/s.

C. Data of analysis

In the following analyses, the major assumptions were made:

- The fluid is a laminar flow

- The fluid flow is incompressible and continuum

- Heat transfer is steady

- Negligible radiation heat transfer.

For the experiments carried out in this study, the effects on the heat transfer and fluid flow – such as heat flux, effectiveness, pressure drop, and performance index – of the heat exchangers will be discussed as follows.

The energy balance equation for the counter-flow microchannel heat exchanger is expressed by:

$$Q_h - Q_{loss} = Q_c = Q \tag{4}$$

Or $$m_h c_h (T_{h,i} - T_{h,o})\eta = m_c c_c (T_{c,o} - T_{c,i}) \tag{5}$$

where Q_h is heat transfer rate of the hot side, Q_c is heat transfer rate of the cold side, Q is actual heat transfer rate, Q_{loss} is heat loss rate from the heat exchanger to the ambient, m is mass flow rate (subscripts h and c stand for the hot side and cold side, respectively), c is specific heat, $T_{h,i}$, $T_{h,o}$, $T_{c,i}$ and $T_{c,o}$ are inlet and outlet temperatures of the hot and cold side, respectively, and η is actual effectiveness.

The maximum heat transfer rate, Q_{max} is evaluated by

$$Q_{max} = (mc)_{min}(T_{h,i} - T_{c,i}) \tag{6}$$

The effectiveness (NTU method) is determined by

$$\varepsilon = \frac{Q_c}{Q_{\max}} \tag{7}$$

Heat flux is calculated by $$q = \frac{Q_c}{A} = \frac{\mathrm{m_c c_c\,(T_{c,o} - T_{c,i})}}{\mathrm{nL_c}W_c} \tag{8}$$

Or $$q = k\Delta T_{lm} = \frac{\Delta T_{lm}}{\Sigma R} \tag{9}$$

The overall thermal resistance ΣR is determined by

$$\Sigma R = R_{cond} + R_{conv} \tag{10}$$

The log mean temperature difference is calculated by

$$\Delta T_{lm} = \frac{\Delta T_{\max} - \Delta T_{\min}}{\ln \dfrac{\Delta T_{\max}}{\Delta T_{\min}}} \tag{11}$$

where m is mass flow rate (subscripts h and c stand for the hot side and cold side, respectively), n is number of microchannels, c is specific heat, $T_{h,i}$, $T_{h,o}$, $T_{c,i}$ and $T_{c,o}$ are inlet and outlet temperatures of the hot and cold sides, respectively, q is heat flux, A is heat transfer area, k is overall heat transfer coefficient, $R_{cond} = \frac{\delta}{\lambda}$ is conductive thermal resistance, $R_{conv} = \frac{1}{h_h} + \frac{1}{h_c}$ is convective thermal resistance, h_h and h_c are the convective heat transfer coefficients of the hot side and the cold sides, respectively, δ is thickness of heat transfer, λ is thermal conductivity, and ΔT_{lm} is the log mean temperature difference.

The Reynolds number is calculated by:

$$\mathrm{Re} = \frac{\rho w D_h}{\mu} = \frac{2m}{\mu (W_c + D_c)} \tag{12}$$

where $D_h = \frac{4A_c}{P}$ is the hydraulic diameter, w is velocity in the z-direction, μ is dynamic viscosity, ρ is density, A_c is cross-sectional area, and P is wetted perimeter.

The total pressure drop of the heat exchanger is given by

$$\Delta p_t = \Delta p_h + \Delta p_c \tag{13}$$

where Δp_h and Δp_c are pressure drops of hot and cold sides, respectively.

The performance index, ξ, is determined by

$$\xi = \frac{Q_c}{\Delta p_t} = \frac{\mathrm{m_c c_c\,(T_{c,o} - T_{c,i})}}{\Delta p_h + \Delta p_c} \tag{14}$$

The experimental uncertainties were estimated, following the method described by Holman [19]; the final expressions for uncertainties were given as follows:

$$\frac{U_{Q_c}}{Q_c}=\left[\left(\frac{\partial m_c}{m_c}\right)^2+\left(\frac{\partial c_c}{c_c}\right)^2+\left(\frac{\partial T_{c,o}+\partial T_{c,i}}{T_{c,o}+T_{c,i}}\right)^2\right]^{1/2} \quad (15)$$

$$\frac{U_{\mathrm{Re}}}{\mathrm{Re}}=\left[\left(\frac{\partial m}{m}\right)^2+\left(\frac{\partial \rho}{\rho}\right)^2+\left(\frac{\partial \mu}{\mu}\right)^2+\left(\frac{\partial W_c}{W_c}\right)^2+\left(\frac{\partial D_c}{D_c}\right)^2\right]^{1/2} \quad (16)$$

$$\frac{U_{\xi}}{\xi}=\left[\left(\frac{\partial m_c}{m_c}\right)^2+\left(\frac{\partial c_c}{c_c}\right)^2+\left(\frac{\partial T_{c,o}+\partial T_{c,i}}{T_{c,o}+T_{c,i}}\right)^2+\left(\frac{\partial \Delta p_h}{\Delta p_h}\right)^2+\left(\frac{\partial \Delta p_c}{\Delta p_c}\right)^2\right]^{1/2} \quad (17)$$

By using the estimated errors of parameters listed in Table 3, the maximum experimental uncertainties in determining Q_c, *Re*, and ξ were 2,1%, 3.1%, and 3.3%, respectively, for all cases being studied.

D. Numerical simulation

Numerical study of the 3D behaviors of heat transfer by the microchannel heat exchangers with single-phase fluid flowing through was done by using the CFD ACE$^+$ software, version 2008.2. The algorithm of this software is based on the finite volume method. For this study, water was used as the working fluid. No internal heat generation is occurred, resulting in Q_i = 0. Nodalization of this model was done by using 172,224 cells and a relative tolerance was 10^{-14}. Fig. 4 shows the convergence of the numerical solver for components of velocity, pressure, and enthalpy.

Number of iteration

Fig. 4. Convergence of the numerical solver

III. RESULTS AND DISCUSSION

A. Numerical results

For the experiments carried out in the study, the inlet temperature and the mass flow rate of the hot side were fixed at 70 ºC and 0.2308 g/s, respectively; at the cold side, the inlet temperature was fixed at 22.5 ºC and the mass flow rates were varying from 0.2135 to 0.401 g/s [20].

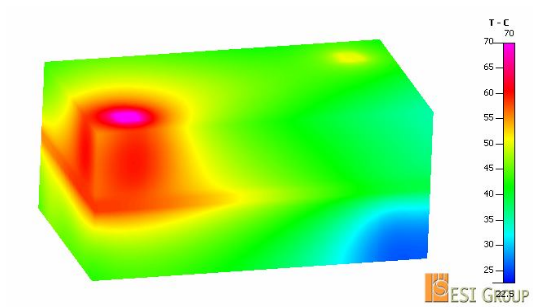

Fig. 5. The temperature profile of the microchannel heat exchanger

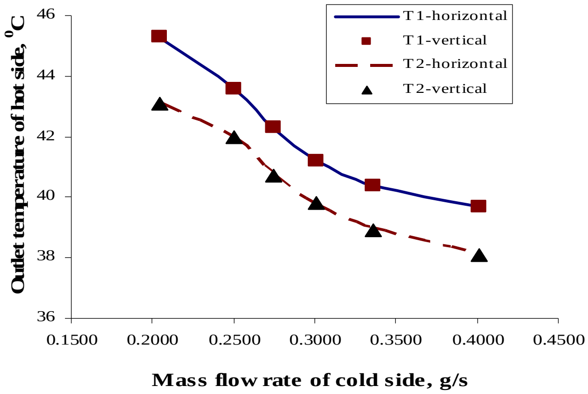

Fig. 6. Numerical comparison of the outlet temperatures of hot side

The thermal boundary conditions of the top and bottom walls of the heat exchanger are assumed to be constant heat flux. The convective heat transfer coefficient between the wall and the ambient used for this solver was 10 W/(m^2K) [18]. The temperature profile of the microchannel heat exchanger T1 is shown in Fig. 5 for the mass flow rate of 0.2135 g/s at the cold side.

Fig. 6 shows a numerical comparison of the outlet temperature of hot side of two microchannel heat exchangers under the effect of gravity. It is observed that the outlet temperatures of hot side obtained from horizontal channels and those from the vertical ones are negligibly small. A numerical comparison of the outlet temperatures of cold side of two microchannel heat exchangers is also shown in Fig. 7. The outlet temperatures (for both the hot and the cold sides) are functions of the mass flow rate of cold side; the outlet temperatures decrease as the mass flow rate of the cold side increases. It is shown from Figs. 6 and 7 that the difference of outlet temperatures obtained from horizontal channels and those from the vertical ones, respectively with T1 and T2, are negligibly small with the maximum percentage error of 0.1%.

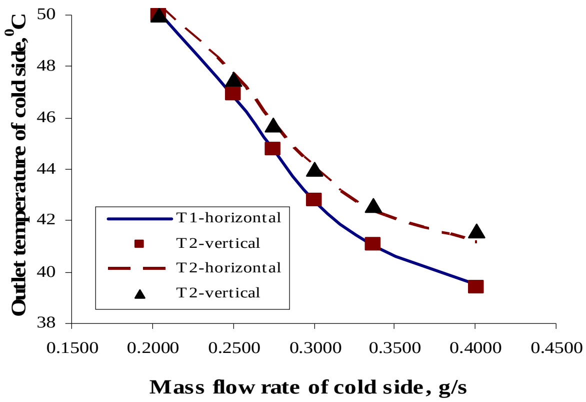

Fig. 7. Numerical comparison of the outlet temperatures of cold side

B. Experimental results

For the experimental system, the inlet temperature and the mass flow rate of the hot side were fixed at 70 ºC and 0.2308 g/s, respectively; at the cold side, the inlet temperature was fixed at 22.5 ºC and the mass flow rates were varying from 0.2135 to 0.401 g/s [20].

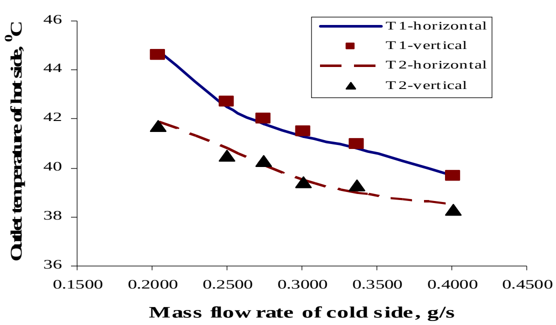

Fig. 8. Experimental comparison of the outlet temperatures of hot side

In this study, influence of gravity was determined by two cases: one with horizontal channels, the other with vertical channels. For vertical channels, the hot water is flowing upward which is against the gravitational field, while the cold water is flowing downward which is in the same direction as the gravitational field. Two microchannel heat exchangers T1 and T2 were tested: these two microchannel heat exchangers have the same physical configurations for their substrates, manifolds, and lengths of channels; only the cross-sectional areas of microchannels are different. The microchannels of T1 have a rectangular cross-section with width of 500 μm and depth of 300 μm; the microchannel of T3, width of 500 μm and depth of 180 μm. Parameters of the heat exchangers (T1 and T2) are listed in more detail in Table 1.

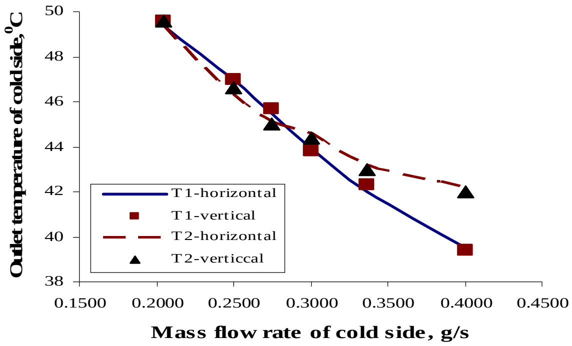

Fig. 9. Experimental comparison of the outlet temperatures of cold side

Experimental comparisons for the outlet temperatures of two microchannel heat exchangers are shown in Figs. 8 and 9 under the effect of gravity. From Figs. 6-9, it is indicated that the numerical results obtaned from Fig. 6 are in good agreement with the experimental results obtained from Fig. 8 and the numerical results obtaned from Fig. 7 are in good agreement with those obtained from Fig. 9. The maximum difference of outlet temperatures for the comparisons in of hot side obtained from horizontal channels and those from the vertical ones are negligibly small, with the maximum percentage of 2.9%.

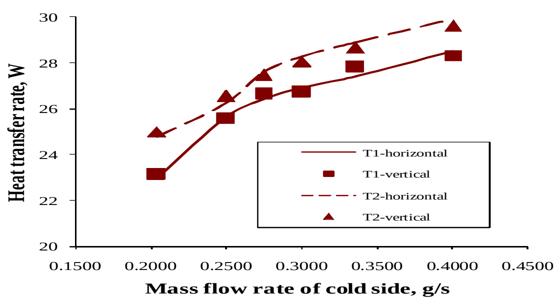

Fig. 10. Experimental comparison of the heat transfer rates

The outlet temperatures of hot side obtained from T1 is higher than those obtained from T2; however, the outlet temperatures of cold side obtained from T1 is lower than those obtained from T2. As a result, the heat transfer rate obtained from T2 is higher than that obtained from T1, as shown in Fig. 10. The results obtained from the present study are in good agreement with those obtained from [9]. Foli et al. [9] indicated that under the constant mass flow rate condition, the higher the heat flux, the lower the aspect ratio (defined as the ratio of the microchannel height to its width).
It is also shown from Fig. 10 that the heat transfer rates obtained from horizontal channels and those from the vertical ones are negligibly small. The heat transfer rate of the heat exchangers is a function of the mass flow rate of cold side: it increases from 24.8 to 29.92 W with the mass flow rate of cold side rising from 0.2043 to 0.401 g/s (for the heat exchanger T2).

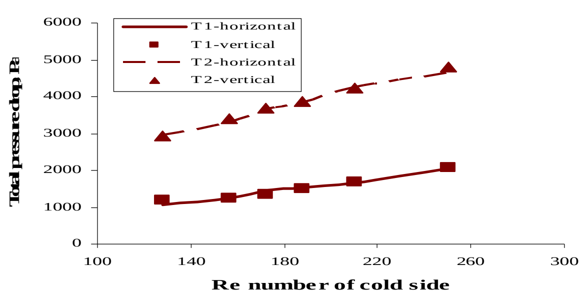

Fig. 11. Experimental comparison of the total pressure drops

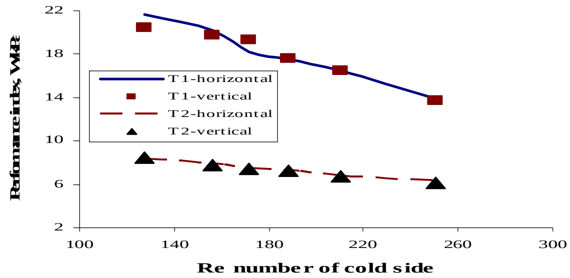

Fig. 12. Experimental comparison of the performance indices

Because that the hydraulic diameter of channel in T2 is smaller than that of channel in T1, this results in the velocity in the channel of T2 to be higher than that of T1, leading to a higher total pressure drop in T2 than that in T1, as shown in Fig. 11. Besides, the Figure shows that the total pressure drop is a function of Reynolds number of cold side; the total pressure drop increases as rising the Re number of cold side.

Experimental results for effects of gravity on the behavior of pressure drop for the microchannel heat exchanger are also shown in Fig. 11. It is observed that the change of pressure drop between the two cases (horizontal channels and vertical channels) is negligibly small; the maximum change in pressure is 7.2% for a pressure drop from 1060 to 2044 Pa.

It was found that the pressure drop of T2 is 2 times higher than that of T1, while the heat transfer rate of T2 is 1.06 times higher than that of T1. As a result, the performance index (defined as the ratio of the heat transfer rate to the pressure drop in the heat exchanger) obtained from T1 is higher than that obtained from T2, as shown in Fig. 12. For heat exchanger T1, a performance index of 21.68 W/kPa was achieved for water from the hot side having an inlet temperature of 70 °C and a mass flow rate of 0.2308 g/s and for water from the cold side having an inlet temperature of 22.5 °C and mass flow rate of 0.2135 g/s. It is also observed that the change of performance between the two cases (horizontal channels and vertical channels) is negligibly small; the maximum change in performance is 5.5%, out of a performance index from 13.69 to 21.68 W/kPa.

A comparison between numerical and experimental results for heat transfer rate with horizontal channels is shown in Fig. 13. It is observed that the numerical results are in good agreement with those obtained from the experimental ones, with the maximum percentage error of 2.94%.

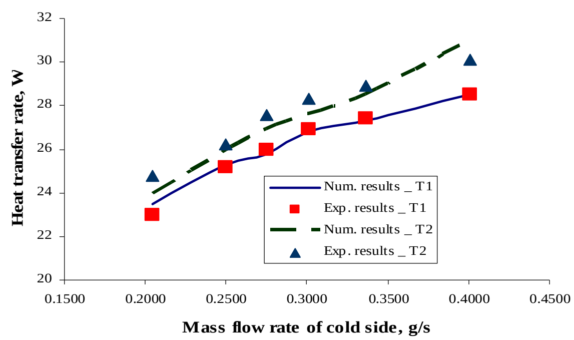

Fig. 13. Comparison of the heat transfer rates between numerical and experimental results with horizontal channels

In summary, it is concluded that the impact of gravity on the fluid flowing through the microchannel heat exchanger can be ignored as indicated in [10-15,17,18,20].

IV. CONCLUSION

Numerical and experimental works were done on two microchannel heat exchangers to carry out the evaluation of their performance for the varying the mass flow rates of the cold side. These two microchannel heat exchangers have the same physical configurations for their substrates, manifolds, and lengths of channels; only the cross-sectional areas of microchannels are different.

For heat exchanger T1, a performance index of 21.68 W/kPa was achieved for water from the hot side having an inlet temperature of 70 °C and a mass flow rate of 0.2308 g/s and for water from the cold side having an inlet temperature of 22.5 °C and mass flow rate of 0.2135 g/s.

The impact of gravity on the fluid through the microchannel heat exchanger was found to be small, with the maximum difference between the results of horizontal and vertical channels being less than 8%. The results obtained from numerical simulations and experimental data are in good agreement. In addition, in this study, good agreements were achieved between the results obtained from the present study and the results obtained from the literatures.

ACKNOWLEDGMENT

The supports of this work by (1) the project (Project No. 54-11-CT/HD-CTTB) sponsored by New Product & Technology Center (NEPTECH) – HCM City Department of Science and Technology of Vietnam, (2) the project (Project Nos. NSC 99-2221-E-033-025 and NSC 100-2221-E-033-065) sponsored by National Science Council of the Republic of China in Taiwan and (3) the project (under Grant No. CYCU-98-CR-ME) sponsored by the specific research fields at Chung Yuan Christian University, Taiwan, are deeply appreciated.

REFERENCES

[1] T.T. Dang, J.T. Teng, and J.C. Chu, Pressure drop and heat transfer characteristics of microchannel heat exchangers: a review of numerical simulation and experimental data, International Journal of Microscale and Nanoscale Thermal and Fluid Transport Phenomena, Vol. 2, Issue 3, 2011

[2] M.P. David, J. Miler, J.E. Steinbrenner, Y.Z. Yang, M. Touzelbaev, K.E. Goodson, Hydraulic and thermal characteristics of a vapor venting two-phase microchannel heat exchanger, International Journal of Heat and Mass Transfer, Volume 54, Issues 25-26, 2011, pp. 5504-5516

[3] J.J. Brandner, L. Bohn, T. Henning, U. Schygulla, and K. Schubert, Microstructure heat exchanger applications in laboratory and industry, Proceedings of ICNMM2006, ICNMM2006-96017, Limerick, Ireland, 2006, pp. 1233-1243

[4] T.A. Ameel, R.O. Warrington, R.S. Wegeng, and M.K. Drost, Miniaturization technologies applied to energy systems, Energy Conversion and Management, Volume 38, 1997, pp. 969–982

[5] G.L. Morini, Single-phase convective heat transfer in microchannels: a review of experimental results, International Journal of Thermal Sciences, Volume 43, Issue 7, 2004, pp. 631-651

[6] B. Mathew and H. Hegab, Application of effectiveness-NTU relationship to parallel flow microchannel heat exchangers subjected to external heat transfer, International Journal of Thermal Sciences, Volume 49, Issue 1, 2010, pp. 76-85

[7] S.W. Kang and S.C. Tseng, Analysis of effectiveness and pressure drop in micro cross-flow heat exchanger, Applied Thermal Engineering, Volume 27, Isuue 5-6, 2007, pp. 877-885

[8] R. Chein and J. Chen, Numerical study of the inlet/outlet arrangement effect on microchannel heat sink performance, International Journal of Thermal Sciences, Volume 48, Issue 8, 2009, pp. 1627-1638

[9] K. Foli, T. Okabe, M. Olhofer, Y. Jin, and B. Sendhoff, Optimization of micro heat exchanger: CFD, analytical approach and multi-objective evolutionary algorithms, International Journal of Heat and Mass Transfer, Volume 49, Issue 5-6, 2006, pp. 1090-1099

[10] T.T. Dang, Y.J. Chang, and J.T. Teng, A study on the simulations of a trapezoidal shaped micro heat exchanger, Journal of Advanced Engineering, Volume 4, Issue 4, 2009, pp. 397-402

[11] T.T. Dang, J.T. Teng, and J.C. Chu, Effect of flow arrangement on the heat transfer behaviors of a microchannel heat exchanger, Proceedings of the International MultiConference of Engineers and Computer Scientists 2010, Hongkong, 2010, pp. 2209-2214

[12] T.T. Dang and J.T Teng, Influence of flow arrangement on the performance index for an aluminium microchannel heat exchanger, IAENG Transactions on Engineering Technologies Volume 5, the American Institute of Physics (AIP), Vol. 1285, 2010, pp. 576-590

[13] T.T. Dang and J.T. Teng, Effect of the substrate thickness of counter-flow microchannel heat exchanger on the heat transfer behaviors, Proceedings of the international symposium on computer, communication, control and automation 2010, Taiwan, 2010, pp. 17-20

[14] T.T. Dang, J.T. Teng, and J.C. Chu, A study on the simulation and experiment of a microchannel counter-flow heat exchanger. Applied Thermal Engineering, Volume 30, Issue 14-15, 2010, pp. 2163-2172

[15] T.T. Dang and J.T. Teng, Comparison on the heat transfer and pressure drop of the microchannel and minichannel heat exchangers, Heat and Mass Transfer, Vol, 47, 2011, pp. 1311-1322

[16] T.T. Dang and J.T. Teng, The effects of configurations on the performance of microchannel counter-flow heat exchangers – An experimental study, Applied Thermal Engineering, Vol. 31, Issue 17-18, 2011, pp. 3946-3955

[17] COMSOL Multiphysics version 3.5 – Documentation, Sept 2008

[18] S.G. Kandlikar, S. Garimella, D.Q. Li, S. Colin, and M.R. King, Heat transfer and fluid flow in minichannels and microchannels. Elsevier, 2006.

[19] J.P. Holman, Experimental methods for engineers, McGraw-Hill, New York, 1984

[20] T.T. Dang, J.T. Teng, and J.C. Chu, Influence of gravity on the performance index of microchannel heat exchangers - Experimental investigations, Lecture Notes in Engineering and Computer Science: Proceedings of The World Congress on Engineering 2011, WCE 2011, 6-8 July, 2011, London, pp. 2094-2099.

Jyh-tong Teng, PhD, PE, is a professor in the Department of Mechanical Engineering and the Senior consultant of the Office of International Affairs at Chung Yuan Christian University (CYCU), Taiwan. He is also the principal investigator of an international education enhancement program sponsored by the Ministry of Education, Republic of China. He received his BS in Mechanical Engineering from Montana State University, MS and PhD in Mechanical Engineering from UC Berkeley. His research areas include thermo-fluidic analyses of compartment fires and smokes, nuclear safety, thermo-fluidics of microchannels, and thermal management of electronic devices.

Thanhtrung Dang, PhD, is a lecturer in the Department of Heat and Refrigeration Technology and the Vice Dean of the Faculty of Automotive Engineering, Hochiminh City University of Technical Education (HCMUTE), Vietnam. He received his BS and MS in the Department of Thermal Technology at Vietnam National University Hochiminh city – Hochiminh city University of Technology (HCMUT), PhD in the Department of Mechanical Engineering, Chung Yuan Christian University (CYCU), Taiwan. His main research interests are nano/microscale heat transfer, energy and sustainable development, industrial refrigeration and air conditioning, and energy economics.

Ngoctan Tran received his BS in the Department of Heat and Refrigeration Technology, Ho Chi Minh City University of Technical Education (HCMUTE), Hochiminh City, Vietnam in 2009. He employed part –time for P.Dussmann Vietnam Co., Ltd as a Supervisor of Engineering from 2008 to 2009, employed full –time for P.Dussmann Vietnam Co., Ltd as a Manager of Laundry Factory from 2009 to 2010, and employed for Darling Electronic – refrigerator Co., Ltd as a technical director in 2010. Presently, he is a master student at Department of Mechanical Engineering, Chung Yuan Christian University, Taiwan. He interested in studying on nano/microscale heat transfer, energy and sustainable development, industrial refrigeration and air conditioning, electronic and control system engineering, and energy economics.